Original Article

Increased Superoxide Radical with a Decrease in Vascular Endothelial Growth Factor and Inducible Nitric Oxide Synthase Level Leads to the Progression of Left Ventricular Hypertrophy in a Pressure-Overload Rat Heart Model

Kaiqiang Ji, MD, PhD, Masahito Minakawa, MD, PhD, Kozo Fukui, MD, PhD, Yasuyuki Suzuki, MD, PhD, and Ikuo Fukuda, MD, PhD

Purpose: This study was designed to evaluate the relationship among free radicals and vascular endothelial growth factor (VEGF) and inducible nitric oxide synthase (iNOS) during the progression of left ventricular hypertrophy (LVH) in pressure-overload rat heart.
Methods: Hypertrophied rat heart created by abdominal aortic banding at the age of 4 weeks was studied at the ages of 14, 15, 18, 21, 26, and 30 weeks (n = 5 in each group). Free radicals were detected by an electron spin resonance (ESR) method using LV tissue. The levels of messenger ribonucleic acid (mRNA) for VEGF, superoxide dismutase (SOD), and iNOS in myocardium were analyzed by reverse transcription (RT)-polymerase chain reaction (PCR).
Results: Free radicals consisting of superoxide families increased over time after aortic banding and were highest in the 30-week group. The SOD mRNA level decreased with the progression of hypertrophy and was inversely proportional to the free radicals level. As compared to the control, the level of mRNA for VEGF and iNOS was significantly increased in 18- and 21-week hypertrophied hearts, but significantly decreased in 26- and 30-week hearts.
Conclusion: The increased level of free radicals with the decrease of VEGF and iNOS levels may contribute to the progression of the pressure-overload hypertrophied heart to the failing heart. (Ann Thorac Cardiovasc Surg 2008; 14: 210–217)

Key words: hypertrophy, free radical, electron spin resonance, vascular endothelial growth factor

Introduction

Myocardial hypertrophy and heart failure are important risk factors of cardiac surgery. The development of hypertrophy is divided into three states: developing hypertrophy, compensatory hypertrophy, and heart failure. In the early state, hypertrophy may be classified as readily reversible physiological hypertrophy. In the longer term, the developing hypertrophy may become beneficial and compensated. Then ultimately the hypertrophy may decay into maladaptive decompensated hypertrophy or heart failure. The identities of signaling pathways that couple the demand for increased contractile power to increased myocyte growth and altered gene expression have been actively studied for many years, but the mechanisms for the transition from compensated to

From Department of Thoracic and Cardiovascular Surgery, Hirosaki University School of Medicine, Hirosaki, Japan

Received March 28, 2007; accepted for publication July 30, 2007
Address reprint requests to Masahito Minakawa, MD, PhD: Department of Thoracic and Cardiovascular Surgery, Hirosaki University School of Medicine, 5 Zaifu-cho, Hirosaki, Aomori 036–8562, Japan.

decompensated heart failure in the hypertrophied heart are poorly known.

Oxidative stress in mitochondria has been widely recognized as an important cause of a variety of diseases, including aging,[1] neurodegeneration,[2,3] and cancer.[4,5] Under certain conditions, such as incomplete oxygen reduction during oxidative phosphorylation, ischemia-reperfusion, and inflammation, the production of reactive oxygen species (ROS) by the mitochondrial electron transport chain can increase several times.[6,7] It is generally thought that some events caused from oxidative stress, such as calcium imbalance, lipid peroxidation, glutathione depletion, and deoxyribonucleic acid (DNA) and protein damage, arise from excessive production of ROS in mitochondria.[8] In the present study, we used electron spin resonance (ESR) to analyze free radicals in the myocardium during the development of left ventricular hypertrophy (LVH) in rat heart.

Vascular endothelial growth factor (VEGF) is a 46-kDa heparin-binding glycoprotein and a specific mitogen for vascular endothelial cells in angiogenesis.[9,10] VEGF induces increased microvascular permeability and monocyte migration through endothelial layers,[11,12] which are important in the processes leading to angiogenesis. Furthermore, VEGF has been shown to increase intracellular calcium and to affect vascular tone-enhanced expression of nitric oxide synthase (NOS), resulting in potent endothelium-dependent relaxation in coronary arteries.[13] The expression of VEGF messenger ribonucleic acid (mRNA) is increased in cardiac myocytes and vascular smooth muscle cells in hypoxia.[14,15] However, little is known about the variety of VEGF involvement in the process leading from developing hypertrophy to heart failure. This study was designed to determine the relationship between oxidative stress and VEGF in the transition from compensated hypertrophied heart to decompensated heart.

Methods

Hypertrophied rat heart model

All animals have received humane care in compliance with the "Principles of Laboratory Animal Care," formulated by the National Society for Medical Research and the "Guide for the Care and Use of Laboratory Animals," prepared by the Institute of Laboratory Animal Resources and published by the National Institutes of Health (NIH Publication No. 86-23, revised 1985). Male Wistar rats (60–70 g, age 4 weeks) were used to create the model of LVH. After anesthesia was induced with intraperitoneal (i.p.) pentobarbital sodium (30 mg/kg), a median laparotomy was performed, and aortic banding was then carried out with a 3-0 silk suture to prevent any stenosis at the descending aorta just above the renal artery.

Thus as the animals grew, the aortic coarctation gradually developed. The LVH group rats were subdivided into 6 groups as follows: 14-week group (14 weeks of age, 10 weeks after banding, $n = 5$), 15-week group (15 weeks of age, 11 weeks after banding, $n = 5$), 18-week group (18 weeks of age, 14 weeks after banding, $n = 5$), 21-week group (21 weeks of age, 17 weeks after banding, $n = 5$), 26-week group (26 weeks of age, 22 weeks after banding, $n = 5$) and 30-week group (30 weeks of age, 26 weeks after banding, $n = 5$). These groups were compared to age-matched control groups that underwent sham operations (control).

Rat myocardium tissue preparation

The rats were anesthetized by i.p. pentobarbital sodium (30 mg/kg), and median laparotomy was done. After the injection of heparin (1,000 U/kg) into the inferior vena cava, the heart was rapidly excised and arrested in ice-cold modified Krebs-Henseleit buffered (KHB) solution. The modified KH solution consisted of the following (in mM): NaCl 118; $NaHCO_3$ 25; glucose 11.1; KCl 4.9; $CaCl_2$ 2.7; $MgSO_4$ 1.2; KH_2PO_4 1.2; and insulin 10 units/liter. After the atrium was removed, the LV was dissected in ice-cold KHB solution and frozen immediately in liquid nitrogen. The ratio of LV to body weight (LV/BW) was used as an index of LVH.

ESR spectroscopy

ESR spectra were obtained at room temperature with a JEOL RE3X ESP spectrometer operating at 9.23 GHz with a 100 kHz modulation frequency. Each sample was set in a TM 110 cavity in liquid nitrogen at temperature 77 K. All measurements were performed with the LV myocardial tissue of LVH and the control group at nonsaturating microwave power of 10 mW. This method can provide a direct method to quantify the generation of free radical within biological tissue. The spectra of free radical were noticed in a receive field at 320 ± 150 mT. The amplitude of each spectrum was measured and normalized as one gram of LV tissue.

Extraction of RNA and reverse transcription-polymerase chain reaction

The total RNA was isolated from rat hearts using an

RNeasy total RNA isolation kit (Qiagen, Germany). reverse transcription (RT) was performed with an RT kit (Promega, USA). One microgram of total RNA was used as a template, and RT-generated complementary DNAs (cDNAs) encoding VEGF and glyceraldehydes-3-phosphate dehydrogenase (G3PDH; internal control), inducible NOS (iNOS), and superoxide dismutase (SOD) were amplified with polymerase chain reaction (PCR). The sequences of the primers for the amplification of cDNA were as follows:

SOD sense:
(5'-GACAAACCTGAGCCCTAAGGG-3')
SOD antisense:
(5'-CTTCTTGCAAACTATG-3')
iNOS sense:
(5'-GCAGTGGAGAGATTTTGCATGAC-3')
iNOS antisense:
(5'-GATGAACTCAATGGCATGAGGC-3')
VEGF sense:
(5'-GAGAATTCGGCCTCCGAAACCATGAACTTTCTGCT-3')
VEGF antisense:
(5'-GAGCATGCCCTCCTGCCCGGCTCACCGC-3')
G3PDH sense:
(5'-TGAACGTCGGGTGTGAACGGATTTGGC-3')
G3PDH antisense:
(5'-CATGTAGGCCATGAGGTCCACCAC-3').

The possible contamination of any PCR component was excluded by performing a PCR reaction with these components in the absence of RT product in each set of experiments (negative control). Twelve microliters of RT-PCR product was checked by using 2% agarose gel electrophoresis containing 0.2 μg/ml ethidium bromide, followed by a photograph under ultraviolet transillumination. The quantification of RNA transcripts was analyzed according to the method described previously, with some modification. The levels of expression of the transcripts were normalized to that of G3PDH mRNA in the same tissue sample. The appropriate number of PCR cycles and the optimal combination of the amount of the first-strand cDNAs were determined for each set of primers to ensure that all PCR reactions were carried out in the linear quantitative phase of the amplification process. The PCR products were fractionated on the agarose gels, visualized by means of ethidium bromide staining, and photographed. The photographs of ethidium bromide-stained gels were scanned with an imaging densitometer linked to a personal computer equipped with image analysis software. The size and optical density of the band produced by the PCR products were quantified by using the Kodak digital science 1-dimensional image analysis software (EDAS 120, Eastman Kodak Co.). For statistical comparison, samples in the experiment were performed to obtain the ratio of density of objective gene to G3PDH mRNA levels.

Statistical analysis

A statistical analysis was performed by one-way analysis of variance (ANOVA), using commercially available software (Statview, Abacus Concepts). All results were presented as mean ± standard error (SE). A value of $P < 0.05$ was considered significant.

Results

Hypertrophied heart model

The LV/BW ratio was used as an index of LV hypertrophy. There was no significant difference in the control group. The ratios in LVH groups were significantly higher than in the control group. The LV/BW ratios in the 18-week and 21-week LVH groups were significantly higher than in other LVH groups. There were no significant differences among 14-, 15-, 26-, and 30-week LVH groups. The SE's of BW, LV wet weight, and whole heart weight of control groups were small, so we think that the BW and heart weight of both groups before aortic banding were almost the same (Table 1).

ESR measurement in hypertrophied heart tissue for free radicals

The ESR signals originated from free radicals were observed around the range of 326.7–328.8 mT in the LV tissue of LVH groups, and these signals were significantly higher than control groups in any age. In LVH groups, signals in the 26- and 30-week LVH groups were significantly higher than in the other LVH groups. The g value was calculated to 2.0022 ± 0.0003, indicating that this signal was derived from free radicals, especially of the superoxide family (Fig. 1). ESR signals in the right ventricle did not differ between control groups and LVH groups (data not shown).

Expression of mRNA for SOD

The expressions of mRNA for SOD showed a significant decrease in LVH groups compared with control groups, and especially the results in 26- (ratio = 0.0359 ± 0.0042) and 30-week LVH groups (ratio = 0.0338 ± 0.0047) were significantly more decreased than the other LVH groups (14-, 15-, 18-, 21-week LVH group ratios

Table 1. Effects of aortic banding on heart mass and body weight

Age (week)	Body weight (kg)		LV wet weight (g)		Whole heart weight (g)		LV/BW ratio	
	Control	LVH	Control	LVH	Control	LVH	Control	LVH
14	0.39 ± 0.04	0.41 ± 0.04	0.80 ± 0.06	1.03 ± 0.15	0.97 ± 0.07	1.22 ± 0.09	1.79 ± 0.13	2.50 ± 0.16*
15	0.42 ± 0.03	0.39 ± 0.08	0.83 ± 0.07	1.14 ± 0.19*	1.01 ± 0.10	1.32 ± 0.16	1.82 ± 0.09	2.65 ± 0.15*
18	0.46 ± 0.05	0.48 ± 0.06	0.91 ± 0.06	1.55 ± 0.15*	1.18 ± 0.09	1.79 ± 0.14*	1.85 ± 0.06	3.36 ± 0.09*†
21	0.48 ± 0.07	0.52 ± 0.02	0.92 ± 0.05	1.56 ± 0.18*	1.21 ± 0.11	1.76 ± 0.17*	1.91 ± 0.07	3.01 ± 0.15*†
26	0.48 ± 0.06	0.48 ± 0.04	0.91 ± 0.08	1.39 ± 0.17*	1.22 ± 0.13	1.56 ± 0.16*	1.92 ± 0.09	2.89 ± 0.18*
30	0.51 ± 0.04	0.53 ± 0.04	0.93 ± 0.06	1.30 ± 0.14*	1.24 ± 0.08	1.60 ± 0.12*	1.90 ± 0.11	2.58 ± 0.16*

BW, body weight; LV, left ventricle; LVH, left ventricular hypertrophied group.
Data are mean ± standard error (SE) (n = 5 each group).
*P <0.05 vs. Control; †P <0.05 vs. 14, 15, 26, 30-week LVH.

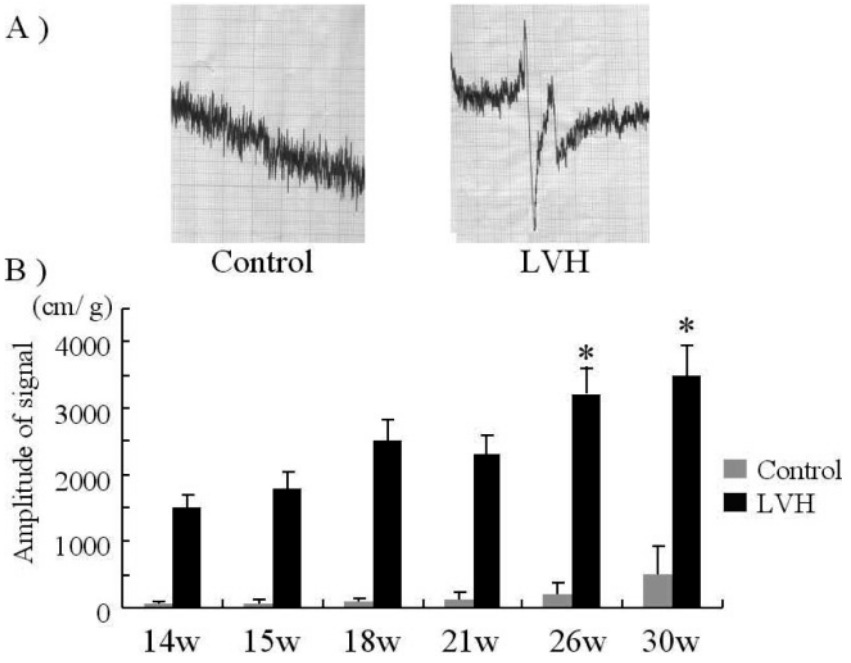

Fig. 1. Free radical signal measured by electron spin resonance (ESR).
A: Signal originated from free radicals were not detected in control group (left figure), while spectrum of free radicals was noticed in a receive field around 326.7–328.8 mT in left ventricular hypertrophy (LVH) group (right figure).
B: The signal from free radicals increased with the progression of LVH. The g value of the signal was calculated at 2.0022 ± 0.0003.
*P <0.05 vs. 14-week LVH group.

were 0.0962 ± 0.0081, 0.0994 ± 0.0054, 0.0764 ± 0.0063, and 0.0667 ± 0.0069, respectively) (Fig. 2). The expression levels in control groups were unchanged throughout.

Expression of mRNA for iNOS

The expression of mRNA for iNOS showed a significant increase in the 18-week LVH group (ratio = 0.192 ± 0.013) and a significant decrease in the 30-week LVH group (ratio = 0.09 ± 0.017) compared with the other LVH groups (14-, 15-, 21-, and 26-week LVH group ratios were 0.128 ± 0.017, 0.142 ± 0.019, 0.155 ± 0.011, and 0.105 ± 0.015, respectively) (Fig. 3). The expression level in control groups was unchanged throughout.

Expression of mRNA for VEGF

The expression of mRNA for VEGF showed a significant increase in the 18-week (ratio = 0.227 ± 0.020) and the 21-week (ratio = 0.236 ± 0.025) LVH groups, and a significant decrease in the 26-week (ratio = 0.111 ± 0.012) and 30-week (ratio = 0.077 ± 0.017) LVH groups compared with the 14-week LVH group (ratio = 0.168 ± 0.018) (Fig. 4). The expression levels in control groups were unchanged throughout.

Discussion

The important finding of this study was that free radicals, especially of the superoxide family, were in-

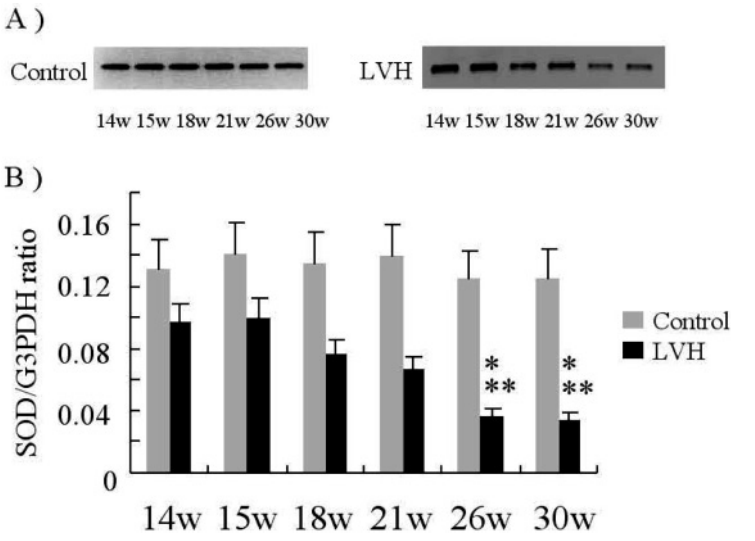

Fig. 2.

A: Expression of messenger ribonucleic acid (mRNA) for superoxide dismutase (SOD) measured by reverse transcriptase (RT)-polymerase chain reaction (PCR).

B: The level of mRNA for SOD in the left ventricular hypertrophy (LVH) groups decreased with the progression of hypertrophy and was significantly low in the 26- and 30-week LVH groups. The level of mRNA for SOD in the control group remained at an equal level.

*P <0.05 vs. control group; **P <0.05 vs. 14-week LVH group.

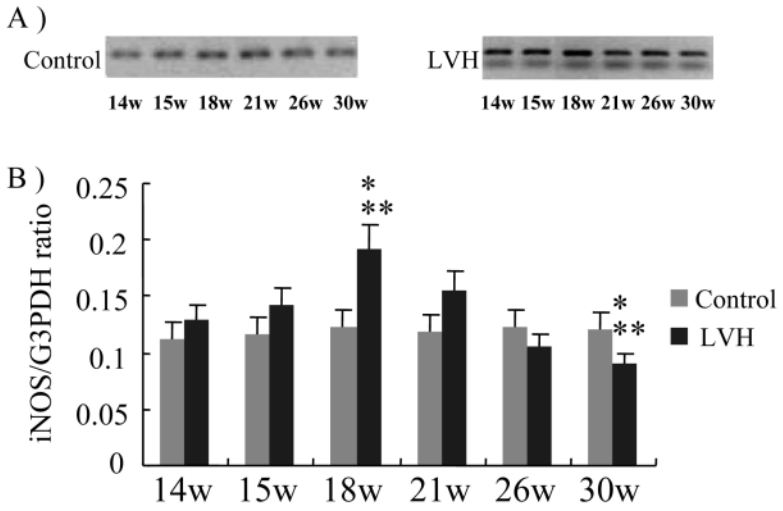

Fig. 3.

A: Expression of messenger ribonucleic acid (mRNA) for inducible nitric oxide synthase (iNOS) measured by reverse transcriptase (RT)-polymerase chain reaction (PCR).

B: The level of mRNA for iNOS in the left ventricular hypertrophy (LVH) group was significantly increased in the 18-week LVH group that is considered to be in a compensated state. However, the level of mRNA for iNOS decreased with the progression to the decompensated state heart and was significantly lower in the 30-week LVH group. The level of mRNA for iNOS in the control group remained at an equal level.

*P <0.05 vs. control group; **P <0.05 vs. 14-week LVH group.

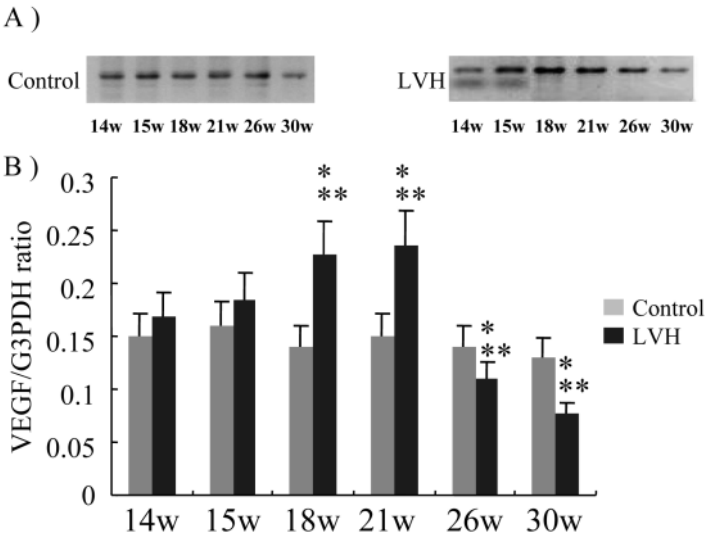

Fig. 4.

A: Expression of messenger ribonucleic acid (mRNA) for vascular endothelial growth factor (VEGF) measured by reverse transcriptase (RT)-polymerase chain reaction (PCR).

B: The level of mRNA for VEGF in the left ventricular hypertrophy (LVH) group was significantly increased in the 18- and 21-week LVH groups that are considered to be in a compensated state. However, the level of mRNA for VEGF decreased with progression to the decompensated state heart and was significantly lower in the 26- and 30-week LVH groups. The level of mRNA for VEGF in the control group remained at an equal level.

*P <0.05 vs. control group; **P <0.05 vs. 14-week LVH group.

creased in developing pressure-overload myocardial hypertrophy. The expressions of VEGF and iNOS mRNA were then increased in the early stage of hypertrophy, but decreased in the late stage.

The LVH models used in this experiment were created by abdominal aortic banding, as we had previously reported,[16] and the LVH had been made a chronic process that evolved from a compensatory state to heart failure. The degree of hypertrophy was assessed with the LV/BW ratio, and it turned out to be 25%–40% increased. It is known that in the transition to heart failure, diastolic dysfunction occurs first and ultimately leads to systolic dysfunction.[17] We have previously observed that by using pressure overload hypertrophied rat heart, created by the same method used in the paper, the minimal rate of contraction ($-dP/dt$) and the isovolumic relaxation time (tau) were significantly lower than the control heart with no deterioration in systolic function at 16 weeks after the operation, whereas both the maximal rate of relaxation ($+dP/dt$) and $-dP/dt$ were significantly deteriorated at 26 weeks after the operation.[16] The LV/BW ratios significantly increased in hypertrophied heart, but in 26- and 30-week groups, the LV/BW ratios were lower, as we previously reported.[16] Moreover, we histologically investigated the hypertrophied heart tissue that we had used in the present study. This revealed that myocardial cells in the LVH groups were hypertrophied, and also in the 21-week LVH group, interstitial fibrosis had begun. In the 30-week LVH group we found obvious interstitial fibrosis and an intricate arrangement of myocardial fiber with necrosis of myocardial cells (data not shown). These findings were not observed in the control group. So it was thought that the reason why the LV/BW ratios with the LV wet weight tended to decrease in the 26- and 30-week LVH groups was a result of fibrous change with myocardial death "apoptosis." The models used in the present study were therefore considered to pathophysiologically represent transition from an early stage of hypertrophied heart (14- and 15-week LVH groups) to the late stage of hypertrophied heart (26- and 30-week LVH groups).

The ESR method for the measurement of free radicals in the myocardial tissue showed that superoxide had increased in the LVH hearts, especially in the myocardium of failing heart. Superoxide comprises many species of free radicals, and because there were different g values measured by ESR, this component appears to be multiplex. Increased superoxide, which is involved in ROS, can cause a deleterious effect on many cell types. The ROS can induce myocardial contractile dysfunction and structural damage.[18] Furthermore, a recent study in isolated cardiac myocytes has shown that a subtle increase in ROS results in a phenotype characterized by hypertrophy and apoptosis that play an important role in myocardial remodeling and heart failure.[19,20] A high level of ROS is produced from a variety of sources, such as the xanthine oxidase system, the leakage of electrons from mitochondria, the cyclooxygenase pathway of arachidonic acid metabolism, and/or the respiratory burst of leukocytes.[21] The major source of free radicals may be from a cleavage of superoxide anion by SOD in mitochondria. The decrease of SOD expression was also validated in the present study.

The expressions of mRNA for iNOS were significantly increased in a compensated state in the 18-week LVH group and decreased in the failing heart state in the present study. It was known that ROS induces the expression of the nuclear factor κ-B (NF-κB) by detaching the inhibitor-κB (I-κB) from the complex of NF-κB and I-κB or inducing the expression of thioredoxin, resulting in various gene expressions, such as cytokines, cell adhesion molecules, and iNOS. However, it has not been revealed what kind of ROS had a major role as those signals. If hydrogen peroxide is the major signal mediator, then in a situation that lacks sufficient intracellular catalase activity, the SOD that catalyzes the reduction of superoxide to hydrogen peroxide will induce the activation of NF-κB, which induces iNOS expression.

We have previously reported that the intracellular level of hydrogen peroxide increased in hypertrophied failing heart, resulting in impaired glycolysis and apoptosis.[22] In the present study, the mRNA level of SOD was significantly decreased in decompensated state (26- and 30-week LVH hearts), thereby indicating the possibility that intracellular SOD was consumed by increased oxygen radicals.

VEGF causes a dose-dependent increase of nitric oxide (NO) concentration in vascular endothelium. In our data, the expressions of mRNA for VEGF and iNOS were parallel. This increase in NO concentration can be demonstrated in vascular segments harvested from different regions, including aorta, vena cava, and pulmonary artery, as well as from cultured human endothelial cells.[23] iNOS, by enhancing diastolic distensibility of the ventricles, might increase preload reserve and thereby support cardiac function under conditions of heart

failure.[24] So the results in the present study showed that NO might increase in the process of LV hypertrophy, especially in the myocardium of compensated hypertrophy, but decrease in the decompensated hypertrophy or heart failure. The concept that iNOS expression might cause heart failure was initially triggered by observations by de Belder et al.,[25] who reported elevated iNOS activities in cardiac biopsy specimens from patients with dilated cardiomyopathy. Later, several studies demonstrated iNOS expressions or activities in hearts from patients with dilated cardiomyopathy, myocarditis, and ischemic cardiomyopathy.[26–28] Based on our data, it is highly unlikely that iNOS may be an important pathological factor in the development of heart failure. Its high level in compensated hypertrophy may be in part responsible for mediating heart failure.

In conclusion, these results suggest that the increased level of free radicals with the decrease of VEGF and iNOS levels may contribute to the progression of the pressure-overload hypertrophied heart to the failing heart.

Acknowledgments

We thank Ryo Miyamoto, Dr. Eng. (Faculty of Science and Technology, Hirosaki University, Hirosaki, Japan) for his helpful cooperation regarding the ESR analysis.

References

1. Wallace DC. Mitochondrial genetics: a paradigm for aging and degenerative diseases? *Science* 1992; **256**: 628–32.
2. Sohal RS, Brunk UT. Mitochondrial production of pro-oxidants and cellular senescence. *Mutat Res* 1992; **275**: 295–304.
3. Cleeter MW, Cooper JM, Darley Usmar VM, Moncada S, Schapira AH. Reversible inhibition of cytochrome c oxidase, the terminal enzyme of the mitochondrial respiratory chain, by nitric oxide. Implications for neurodegenerative diseases. *FEBS Lett* 1994; **345**: 50–4.
4. Hennet T, Richter C, Peterhans E. Tumour necrosis factor-alpha induces superoxide anion generation in mitochondria of L929 cells. *Biochem J* 1993; **289** (Pt 2): 587–92.
5. Hennet T, Bertoni G, Richter C, Peterhans E. Expression of BCL-2 protein enhances the survival of mouse fibrosarcoid cells in tumor necrosis factor-mediated cytotoxicity. *Cancer Res* 1993; **53**: 1456–60.
6. Flaherty JT, Weisfeldt ML. Reperfusion injury. *Free Radic Biol Med* 1988; **5**: 409–19.
7. Janssen YM, Van Houten B, Borm PJ, Mossman BT. Cell and tissue responses to oxidative damage. *Lab Invest* 1993; **69**: 261–74.
8. Richter C, Gogvadze V, Laffranchi R, Schlapbach R, Schweizer M, et al. Oxidants in mitochondria: from physiology to diseases. *Biochim Biophys Acta* 1995; **1271**: 67–74.
9. Connolly DT, Heuvelman DM, Nelson R, Olander JV, Eppley BL, et al. Tumor vascular permeability factor stimulates endothelial cell growth and angiogenesis. *J Clin Invest* 1989; **84**: 1470–8.
10. Connolly DT, Olander JV, Heuvelman D, Nelson R, Monsell R, et al. Human vascular permeability factor. Isolation from U937 cells. *J Biol Chem* 1989; **264**: 20017–24.
11. Senger DR, Perruzzi CA, Feder J, Dvorak HF. A highly conserved vascular permeability factor secreted by a variety of human and rodent tumor cell lines. *Cancer Res* 1986; **46**: 5629–32.
12. Clauss M, Gerlach M, Gerlach H, Brett J, Wang F, et al. Vascular permeability factor: a tumor-derived polypeptide that induces endothelial cell and monocyte procoagulant activity, and promotes monocyte migration. *J Exp Med* 1990; **172**: 1535–45.
13. Sellke FW, Wang SY, Stamler A, Lopez JJ, Li J, et al. Enhanced microvascular relaxations to VEGF and bFGF in chronically ischemic porcine myocardium. *Am J Physiol* 1996; **271**: H713–20.
14. Ladoux A, Frelin C. Hypoxia is a strong inducer of vascular endothelial growth factor mRNA expression in the heart. *Biochem Biophys Res Commun* 1993; **195**: 1005–10.
15. Brogi E, Wu T, Namiki A, Isner JM. Indirect angiogenic cytokines upregulate VEGF and bFGF gene expression in vascular smooth muscle cells, whereas hypoxia upregulates VEGF expression only. *Circulation* 1994; **90**: 649–52.
16. Minakawa M, Takeuchi K, Ito K, Tsushima T, Fukui K, et al. Restoration of sarcoplasmic reticulum protein level by thyroid hormone contributes to partial improvement of myocardial function, but not to glucose metabolism in an early failing heart. *Eur J Cardiothorac Surg* 2003; **24**: 493–501.
17. Yamakado T, Nakano T. Left ventricular systolic and diastolic function in the hypertrophied ventricle. *Jpn Circ J* 1990; **54**: 554–62.
18. Josephson RA, Silverman HS, Lakatta EG, Stern MD, Zweier JL. Study of the mechanisms of hydrogen peroxide and hydroxyl free radical-induced cellular injury and calcium overload in cardiac myocytes. *J Biol Chem* 1991; **266**: 2354–61.
19. Siwik DA, Tzortzis JD, Pimental DR, Chang DL, Pagano PJ, et al. Inhibition of copper-zinc superoxide dismutase induces cell growth, hypertrophic phenotype, and apoptosis in neonatal rat cardiac myocytes in vitro. *Circ Res* 1999; **85**: 147–53.
20. Sawyer DB, Colucci WS. Mitochondrial oxidative stress in heart failure: "oxygen wastage" revisited.

Circ Res 2000; **86**: 119–20.
21. McCord JM. Oxygen-derived radicals: a link between reperfusion injury and inflammation. *Fed Proc* 1987; **46**: 2402–6.
22. Itoh K, Takeuchi K, Minakawa M, et al. Role of oxidative stress in transition of hypertrophied myocardium to heart failure. In: Munakata A ed.; Progress in Transplantation. Amsterdam: Elsevier Science B.V., 2000; pp 33–40.
23. van der Zee R, Murohara T, Luo Z, Zollmann F, Passeri J, et al. Vascular endothelial growth factor/vascular permeability factor augments nitric oxide release from quiescent rabbit and human vascular endothelium. *Circulation* 1997; **95**: 1030–7.
24. Heymes C, Vanderheyden M, Bronzwaer JG, Shah AM, Paulus WJ. Endomyocardial nitric oxide synthase and left ventricular preload reserve in dilated cardiomyopathy. *Circulation* 1999; **99**: 3009–16.
25. de Belder AJ, Radomski MW, Why HJ, Richardson PJ, Martin JF. Myocardial calcium-independent nitric oxide synthase activity is present in dilated cardiomyopathy, myocarditis, and postpartum cardiomyopathy but not in ischaemic or valvar heart disease. *Br Heart J* 1995; **74**: 426–30.
26. Haywood GA, Tsao PS, von der Leyen HE, Mann MJ, Keeling PJ, et al. Expression of inducible nitric oxide synthase in human heart failure. *Circulation* 1996; **93**: 1087–94.
27. Drexler H, Kästner S, Strobel A, Studer R, Brodde OE, et al. Expression, activity and functional significance of inducible nitric oxide synthase in the failing human heart. *J Am Coll Cardiol* 1998; **32**: 955–63.
28. Paulus WJ, Kästner S, Pujadas P, Shah AM, Drexler H, et al. Left ventricular contractile effects of inducible nitric oxide synthase in the human allograft. *Circulation* 1997; **96**: 3436–42.